FGF Signaling Is Essential for Ophthalmic Trigeminal Placode Cell Delamination and Differentiation

Rhonda N.T. Lassiter[†], **Stephanie B. Reynolds**[†], **Kristopher D. Marin**, **Tyler F. Mayo**, and **Michael R. Stark**[*]

Department of Physiology and Developmental Biology, Brigham Young University, Provo, Utah

Abstract

The ophthalmic trigeminal (opV) placode gives rise exclusively to sensory neurons of the peripheral nervous system, providing an advantageous model for understanding neurogenesis. The signaling pathways governing opV placode development have only recently begun to be elucidated. Here, we investigate the fibroblast growth factor receptor-4 (FGFR4), an opV expressed gene, to examine if and how FGF signaling regulates opV placode development. After inhibiting FGFR4, Pax3+ opV placode cells failed to delaminate from the ectoderm and did not contribute to the opV ganglion. Blocking FGF signaling also led to a loss of the early and late neuronal differentiation markers Ngn2, Islet-1, NeuN, and Neurofilament. In addition, without FGF signaling, cells that stalled in the ectoderm lost their opV placode-specific identity by down-regulating Pax3. We conclude that FGF signaling, through FGFR4, is necessary for delamination and differentiation of opV placode cells.

Keywords

FGF; FGFR4; Pax3; ophthalmic trigeminal placode; sensory neurogenesis; chicken

Introduction

Sensory neurons of the cranial ganglia are derived from two distinct cell populations, the neurogenic placodes and a subset of neural crest cells (D'Amico-Martel and Noden, 1983). Among the neurogenic placodes, only the trigeminal and epibranchial placodes give rise exclusively to sensory neurons, while others such as the olfactory and otic placodes generate multiple derivatives (reviewed in Baker and Bronner-Fraser, 2001; Schlosser, 2006). The trigeminal and epibranchial placodes provide a valuable model for investigating the necessary elements of sensory neurogenesis. The trigeminal ganglion, the sensory ganglion of cranial nerve V, consists of the ophthalmic (opV) and the maxillomandibular (mmV) branches, with each branch originating from its corresponding unique placode. Both placodes contribute sensory neurons to their respective ganglionic lobes, while the neural crest contributes both sensory neurons as well as glial cells (reviewed in Baker and Bronner-Fraser, 2001; Schlosser, 2006).

Trigeminal ganglion development begins as zones of ectodermal cells from the preplacodal domain are specified into individual placodes (Streit, 2004). Induction of the opV placode occurs as competent ectoderm receives a diffusible signal from the midbrain–hindbrain region

of the neural tube. Specification has been shown to coincide with protein expression of the transcription factor Pax3, the earliest known molecular marker of the opV placode. These Pax3-positive cells delaminate from the surface ectoderm, migrate through the mesenchyme, condense with neural crest cells, and continue differentiating into cutaneous sensory neurons of the opV branch of the trigeminal ganglion (Stark et al., 1997; Baker et al., 1999, 2002). Although the cellular processes and tissue interactions of opV placode development have been understood for some time, only recently have the signaling pathways involved begun to be elucidated. In 2007, we presented evidence that canonical Wnt signaling is required for maintenance and possibly induction of Pax3 expression, and the expression of other opV placode, pan-placodal, and neuronal differentiation markers. Canonical Wnt signaling, however, is not sufficient alone to induce the opV placode cell fate (Lassiter et al., 2007). This study demonstrated that canonical Wnt signaling was crucial throughout early development of opV sensory neurons. McCabe and Bronner-Fraser (2008) showed that platelet-derived growth factor (PDGF) is necessary for induction of the opV placode and is sufficient to increase the number of opV neurons in the condensing ganglion. They also concluded that PDGF signaling could not specify opV placode cells independently, but likely required additional cofactors. More recently it was reported that coordinated Wnt and FGF signaling from the midbrain–hindbrain region of the neural tube was necessary and sufficient for the formation and differentiation of the opV placode (Canning et al., 2008).

In this study, we investigate the function of the fibroblast growth factor (FGF) signaling pathway in opV placode development. The FGF receptor-4 (FGFR4) is expressed in the opV placode beginning in a subset of Pax-3–expressing placode cells at the 10 somite stage (ss), with peak expression occurring throughout the 15–28 ss, when the majority of placode cells are delaminating from the surface ectoderm (Marcelle et al., 1994; Stark et al., 1997; Xu et al., 2008). FGFR4 expression is short-lived in opV placode cells, in that mRNA can only be detected within a subset of placodal ectoderm cells, and in newly delaminated cells. Expression is down-regulated in migratory placode cells, and is not detected in the condensed trigeminal ganglion (Stark et al., 1997). The transient spatiotemporal expression of FGFR4 lends to the hypothesis that FGF signaling may regulate opV placode cell delamination.

FGF signaling has also been shown to play a crucial role in the development of many other placodes. In 2006, Bailey et al. presented data in chick indicating that FGF8, emanating from the anterior neural ridge, restricts specification of the lens fate and in turn promotes olfactory placode formation. Studies have also shown that in chick and zebrafish, FGFs are crucial for induction of both the epibranchial and otic placodes (Ladher et al., 2005; Martin and Groves, 2006; Sun et al., 2007; Nechiporuk et al., 2007; Nikaido et al., 2007; Freter et al., 2008). Here, we identify an essential role for FGF signaling in delamination and differentiation of the ophthalmic trigeminal placode. Through inhibition of FGFR4, we find that opV cells no longer delaminate, become stalled in the ectoderm, fail to differentiate, and eventually lose their opV placode identity.

Results

FGF Signaling Is Essential for opV Placode Cell Delamination

The initial expression of FGFR4 mRNA within the ophthalmic trigeminal (opV) placode domain occurs shortly after Pax3 expression and is not maintained in the differentiating ganglion (Stark et al., 1997). This transient expression of FGFR4 suggests a role for FGF signaling in delamination of Pax3+ opV cells from the surface ectoderm. To determine whether FGF signaling is necessary for opV placode cell development, we used a previously described secreted-FGFR4 misexpression construct (sFGFR4; Marics et al., 2002), which acts to inhibit FGF signaling by expressing only the extracellular region (the first ~860 coding base pairs) of the molecule, thereby competing away endogenous FGF ligand. The sFGFR4 construct was

shown to specifically inhibit FGFR4 signaling in limb myogenesis, and because it does not include a transmembranal segment, does not heterodimerize with other FGF receptors (Marics et al., 2002). The sFGFR4 expression vector or control GFP vector was electroporated into the cranial ectoderm of 7–9 ss chick embryos, before significant endogenous FGFR4 expression and just before or at the onset of cellular delamination, and collected 24, 30, and 36 hr after electroporation. Embryos were prepared for immunohistochemistry as described, and sections through the opV placode/ganglion region were analyzed to characterize green fluorescent protein–positive (GFP+) -targeted cells within the opV domain. Placodes/ganglia targeted on both sides of the same embryo were analyzed independently (n = number of placodes or ganglia), with all data sets containing a minimum of five embryos.

In initial experiments, embryos were allowed to develop 36 hr after electroporation (approximately the 31–33 ss), when the majority of opV placode cells have migrated and condensed in the ganglion. The cellular effects were quantified by counting the number of targeted opV cells that delaminated from the cranial ectoderm and contributed to the opV ganglion. In GFP-electroporated control embryos, numerous Pax3+/GFP+ cells were found within the ganglion (Fig. 1A,B,D), whereas sFGFR4-GFP experimental embryos showed a dramatic loss of Pax3+/GFP+ cells in the mesenchyme and ganglion (Fig. 1F,G,I), with the vast majority of targeted cells remaining in the ectoderm. Quantitative analysis of the number of Pax3+/GFP+ cells (normalized for total Pax3+ cells in the ganglion to account for developmental stage differences) showed a significant difference between control vs. experimental embryos. In GFP-control embryos the mean percentage of Pax3+ ganglionic cells that coexpressed GFP was 46.2% (SEM ± 4.87, n = 8) vs. 6.71% (SEM ± 1.08, n = 9) for sFGFR4 experimental embryos. Therefore, inhibition of FGFR4 in the opV placode led to a highly statistically significant reduction of targeted opV cells delaminating and contributing to the ganglion ($P < 0.0001$; Fig. 1K). Of interest, although targeted opV placode cells in experimental embryos did not contribute to the ganglion, the opV ganglion still contained similar numbers of Pax3+/GFP− placode cells, indicating that untargeted ectoderm retains placodal competence at early stages, and any non–cell-autonomous effect by sFGFR4 was not significant. Having observed a significant reduction in targeted cells contributing to the ganglion after sFGFR4 expression, we next analyzed targeted cells that remained in the ectoderm. In both control and experimental embryos at the 31–33 ss, broad GFP expression was observed in the ectoderm. Control embryos showed a few Pax3+/GFP+ cells still remaining in the ectoderm, although the majority had delaminated. Surprisingly, in experimental embryos the same result was observed with only a few Pax3+/GFP+ cells found in the ectoderm. The vast majority of sFGFR4-targeted cells observed did not undergo delamination, but remained in the ectoderm and did not continue to express the opV marker Pax3 36 hr after electroporation (31–33 ss; Fig. 1F–J).

To further investigate the time course of Pax3 down-regulation, and to ensure that initial Pax3 expression was not being blocked by sFGFR4, we repeated electroporations and analyzed embryos at 24 (~24 ss, Fig. 2) and 30 hr (~28 ss, data not shown) after electroporation. sFGFR4 (n = 6) or GFP (n = 6) embryos 24 hr after electroporation showed no difference in the number of targeted Pax3+ cells in the ectoderm ($P < 0.40$). Both GFP (Fig. 2A–E) and sFGFR4 (Fig. 2F–J) embryos showed many coexpressing targeted GFP+/Pax3+ cells in the placodal ectoderm. Furthermore, sFGFR4 embryos (n = 10) 30 hr after electroporation had similar numbers of GFP+/Pax3+ coexpressing ectodermal cells when compared with GFP control embryos (n = 10). However, 28 ss embryos (both experimental and controls) had many fewer Pax3+-targeted cells in the ectoderm when compared with 24 ss embryos. From these and prior observations, we find that during normal development many Pax3+ opV placode cells reside in the ectoderm at the 24 ss, with cells continually delaminating and entering the mesenchyme. The majority of Pax3+ cells will have left the ectoderm by the 32 ss, and maintained Pax3 expression through ganglion formation. In sFGFR4 electroporated embryos, ectodermal Pax3

+ opV placode cells followed a similar time course of initial Pax3 expression, however when the cells failed to delaminate, Pax3 was down-regulated in the targeted cells now stalled in the ectoderm.

Although sFGFR4 can potentially produce a non–cell-autonomous effect by sequestering available ligand, our data did not support this. However, to verify secreted FGFR4 data and to determine whether there were any unrealized non–cell-autonomous effects from the secreted FGFR4, we repeated electroporations using a cytoplasmic truncated FGFR4 (tFGFR4) construct. The tFGFR4 gene includes the transmembranal segment which anchors the receptor to the cell-membrane thereby producing a cell-autonomous effect. Experiments using tFGFR4 generated comparable inhibition and confirmed the sFGFR4 data (see Supp. Fig. S1, which is available online).

To ensure specificity of FGF inhibition, we used an independent approach of blocking FGF signaling using the chemical inhibitor SU5402 (an FGF receptor antagonist). The 15 ss chick embryo heads were cultured with the addition of SU5402 (50 μM) or dimethyl sulfoxide (DMSO) for 18 hr, during the time of peak delamination. Embryo heads were sectioned and immunostained for Pax3 and Islet1 protein (Fig. 3A–D). Pax3+ placode cells in the mesenchyme were counted from five random sections to determine the number of delaminated opV placode cells. Analysis revealed a significant decrease in the total number of mesenchyme cells from SU5402 head cultures (43.0; SEM ± 11.4; n = 9) when compared with DMSO controls (75.14; SEM ± 21.3; n = 7), a difference of 32.14 cells/placode ($P < 0.01$; Fig. 3E). These data support the sFGFR4 experiments showing an obvious decrease of opV placode cell delamination when the FGF signaling pathway is blocked.

FGF Signaling Is Necessary for Differentiation

To determine whether ectodermal sFGFR4-targeted opV cells still retain the capacity to differentiate as neurons, we analyzed the expression of both early and late neuronal markers. Ngn2 is one of the earliest neuronal markers and is strongly up-regulated in opV ectoderm (Perez et al., 1999; Begbie et al., 2002). Embryos (7–9 ss) were electroporated with sFGFR4 and analyzed 24 hr after electroporation for *Ngn2* mRNA expression by whole-mount in situ hybridization. Experimental embryos showed a clear reduction or loss of *Ngn2* expression (6/8 placodes; Fig. 4E–H) in the opV placode compared with controls, where strong *Ngn2* expression was always observed (10/10 placodes; Fig. 4A–D). It is possible that *Ngn2* is briefly up-regulated, and then lost in response to sFGFR4 misexpression because some targeted cells did show *Ngn2* expression.

Unlike Ngn2, Islet-1 is an early neuronal differentiation marker (Ericson et al., 1992; Mulder et al., 1995) that is expressed primarily in opV cells as they begin to enter the mesenchyme (although a few ectodermal cells also express Islet-1), with continued expression in the developing opV ganglion. Islet-1, therefore, marks a later stage of neuronal differentiation than does *Ngn2*. Electroporations were performed as described above. Embryos were analyzed for Islet-1 expression at 24 (~24 ss, Fig. 2) and 36 (~32 ss, Fig. 1) hr after electroporation. Targeted sFGFR4 ectodermal cells had down-regulated Pax3 and did not express Islet-1 36 hr after electroporation (Fig. 1F,H,J), although the few targeted cells that did contribute to the ganglion did express both Pax3 and Islet-1. Because there is approximately a 3- to 4-hr delay in ectopic gene expression after electroporation, a few targeted cells likely will have escaped the ectoderm just before ectopic expression of sFGFR4 protein. We suspect that the few cells found in the ganglion are these early-escaping cells, indicating the need for FGFR4 function in opV placode cells is indeed transient. Untargeted Pax3+ cells in the mesenchyme and ganglion expressed Islet-1 in a normal manner comparable to GFP-targeted controls (Fig. 1A,C,E). Analysis of embryos 24 hr after electroporation with sFGFR4 or GFP (approximately the 24 ss, when many of the targeted cells still maintained Pax3 expression) showed that, within the ectoderm, Islet-1

was rarely expressed in sFGFR4-expressing GFP+/Pax3+ cells (Fig. 2F–J) and that this ectodermal expression was not significantly different from GFP controls (Fig. 2A–E). Therefore, targeted ectoderm cells do not increase expression of the early differentiation marker Islet-1 at 24 or 36 hr after electroporation. SU5402 experiments also showed that, although placode cell delamination was dramatically reduced, Pax3+ cells did not up-regulate Islet-1 in the ectoderm (Fig. 3B,D).

To ensure that neuronal differentiation was not occurring in sFGFR4 cells that remained in the ectoderm, we also analyzed expression of the late neuronal differentiation markers NeuN (neuronal-specific nuclear protein; Mullen et al., 1992) and Neurofilament. Embryos were electroporated as before and allowed to develop for 36 hr to the 31–33 ss. As in earlier experiments, the vast majority of sFGFR4-targeted cells remained in the ectoderm, and although the neuronal markers were still expressed in the cells of the opV ganglion, targeted cells in the ectoderm did not up-regulate Neurofilament (n = 5; Fig. 5A–D) or NeuN (n = 5; Fig. 5E–H). These data indicate that sFGFR4 expression prevented opV placode cellular delamination, and cells that failed to escape the ectoderm also failed to differentiate as neurons.

FGF Inhibition Does Not Allow opV Cells to Acquire the Fate of Other Nearby Placodes

Throughout all stages and time points tested, the vast majority of sFGFR4-targeted cells remain in the ectoderm and eventually down-regulate Pax3, seemingly losing their opV-specific identity. Although FGF signaling is required for the induction of surrounding placodes (Faber et al., 2001; Martin and Groves, 2006; Sun et al., 2007; Nechiporuk et al., 2007; Nikaido et al., 2007; Freter et al., 2008), we next wanted to address the possibility that inhibiting FGFR4 in opV cells may allow them to adopt a different placodal fate or even perhaps revert back to the lens placode ground state of all sensory placodes (Bailey et al., 2006). We analyzed sFGFR4 electroporated embryos 36 hr after electroporation for the expression of Pax2, which marks the epibranchial as well as the otic placodes in the chick (Baker and Bronner-Fraser, 2000), and Pax6, which marks the lens placode (Bailey et al., 2006; Bhattacharyya et al., 2004). Immunohistochemistry on sections through the head region showed that sFGFR4-targeted cells did not up-regulate Pax2 (n = 5; Fig. 6A–D) or Pax6 (n = 5; Fig. 6E–H) in any of the embryos tested. However, targeted cells in the presumptive lens ectoderm, adjacent to the opV placode, did continue to express Pax6 (Fig. 6G,H).

Blocking FGF Signaling Does Not Alter the Proliferative State of head opV Ectoderm

To further investigate the fate of sFGFR4-targeted opV placode cells, we assayed the cells for incorporation of bromodeoxyuridine (BrdU) to analyze their proliferative state. Electroporations on 7–9 ss embryos were performed as previously described. Embryos were allowed to develop 35 hr after electroporation, when 50–75 μl of BrdU was applied to the embryo surface. Embryos were incubated for an additional 1 hr before collection. Sections were stained with Pax3, BrdU, and DAPI (4′,6-diamidine-2-phenylidole-dihydrochloride; Fig. 7A–H). BrdU+ and DAPI+ ectodermal cells were analyzed in the targeted opV placode defined by GFP and Pax3 expression. The average percentage of BrdU+/DAPI+ cells in control vs. experimentals revealed that proliferation of targeted cells continued in opV ectoderm. In control embryos, an average of 33.2% (SEM ± 2.9; n = 6) of ectodermal cells were BrdU+, similar to experimental embryos with 34.1% (SEM ± 2.8; n = 5), resulting in no significant difference ($P < 0.84$; Fig. 7I).

FGF8 Misexpression Alone Does Not Increase Delamination or Differentiation

FGF8 is secreted from the midrain–hindbrain boundary adjacent to the opV placode (Crossley et al., 1996; Canning et al., 2008). To test the effect of increased FGF signaling on placodal delamination and differentiation we misexpressed FGF8 in ectoderm from the forebrain to the first somite. Embryos were electroporated (7–9 ss) as previously described with FGF8 and

allowed to develop 24 and 36 hr after electroporation. Embryos collected at 24 hr did not show an increase in Pax3 cells or delaminating cells into the mesenchyme compared with controls (Supp. Fig. S2A–E; compare with Fig. 2 controls). Embryos harvested at 36 hr did not show evidence of ectopic ganglia or an increase in the number of GFP or Pax3 cells contributing to the opV trigeminal ganglion (Supp. Fig. S2F–J; compare with Fig. 1 controls).

Discussion

FGFR4 is robustly expressed in the chick opV placode during a time coincident with placode cell delamination from the surface ectoderm. To test the hypothesis that FGFR4 regulates opV placode cell delamination, we inhibited FGF signaling by electroporating secreted FGFR4, which expresses only the extracellular region of the gene and competes away endogenous ligand. Our results clearly demonstrate that blocking FGF signaling at this critical time point in placode development results in a dramatic decrease in targeted Pax3+ cells entering the mesenchyme and contributing to the ganglion. We also show that targeted cells remain in the ectoderm and do not differentiate as ectopic neurons or adopt a different placodal identity, as assayed by markers of surrounding placodes, including epibranchial, otic, and lens. Finally, we explored the possibility that targeted cells show unique proliferative states, such as those observed in stem-like progenitor cells. BrdU labeling after sFGFR4 misexpression, however, did not reveal an increase or decrease in cell proliferation. These results show that activation of FGF-FGFR4 signaling is a crucial step in opV placode cell delamination and differentiation.

While the results clearly show a failure of cellular delamination, a delayed loss of placode markers, and a loss of differentiating neurons, it is difficult to assess whether the effect of blocking FGF signaling directly regulates one cellular process, multiple processes, or whether the processes of delamination and differentiation are inseparably linked in opV placode cells. One recent study showed that FGF signaling may modulate cytoskeletal rearrangements of epithelial cells (Sai and Ladher, 2008). FGF signaling may likewise work through similar pathways in regulating delamination of opV ectoderm cells. Although it is possible that FGFR4 signaling plays a role in both delamination and neuronal differentiation, our data may support an interpretation wherein FGFR4 regulates only delamination, and that this cellular process is required for subsequent neuronal differentiation. It is particularly compelling that sFGFR4-targeted cells that escape the ectoderm (presumably because they delaminated just after electroporation but before transgene up-regulation) go on to differentiate within the opV ganglion, while cells stalled in the ectoderm do not. Continual FGFR4, or FGF signaling in general, cannot therefore be needed for differentiation after cellular delamination, only before and/or during. Understanding the cell–cell adhesion and cellular migration mechanisms working in the placodes would reveal much about the link between delamination and differentiation.

Conversely, if FGFR4 signaling only regulates delamination, it would be expected that sFGFR4-targeted cells remaining in the ectoderm would retain the ability to differentiate, producing ectopic ganglia. Evidence of trigeminal ectopic ganglia has previously been found in the surface ectoderm of chick embryos. These aberrant ectodermal ganglia expressed neurofilament protein, possessed neurites that associated with the ophthalmic nerve, and showed neuronal morphological characteristics (Kuratani and Hirano, 1990). Here, we demonstrate that both cellular delamination and neuronal differentiation are blocked after sFGFR4 expression. We show that, after a certain time point in development, between 24 and 32 somites, targeted cells that are stalled in the ectoderm down-regulate Pax3, losing their opV-specific placode identity. Thus, specified opV placode cells can maintain placode identity for a time even in the absence of FGF signaling, but they eventually lose that identity. This may be similar to what has been observed in the epibranchial placodes, where cells are released from the surface ectoderm as neuroblasts (not as undifferentiated mesenchymal cells) that then

go on to differentiate after delamination (Graham et al., 2007). As another example of Pax3/ FGFR4 regulation of cellular differentiation, in limb bud myogenesis muscle progenitor cells express Pax3 and migrate into the limb bud from the lateral dermomyotome. These Pax3+ cells delaminate and migrate without FGFR4, but require FGFR4 for muscle differentiation (Marics et al., 2002). Therefore, the data presented here could be interpreted to support FGFR4 being additionally required for neuronal differentiation of opV placode cells. Uncoupling the processes of delamination and differentiation in opV placode development may not be possible without disturbing developmental progression, and in fact these processes may be tightly linked. Ge et al. (2006) found that proneural basic helix–loop–helix (bHLH) genes such as Ngn2 promoted neuronal differentiation *and* enhanced cellular migration in cultured neural progenitor cells (NPCs). They demonstrated that different mutant forms of bHLH proteins either lose their ability to induce neurogenesis but retain their ability to induce cell migration, or retain their ability to induce neurogenesis but lose their ability to induce cell migration. They concluded that bHLH genes serve as molecular "linkers" of neurgenesis and migration, and that target genes ultimately require multiple transcriptional activators to modulate gene expression and cellular processes (Ge et al., 2006). From our results, blocking FGF signaling resulted in down-regulation of the bHLH gene *Ngn2*, demonstrating that FGFR4 likely plays a key role in regulating the expression of neurogenesis genes and in modulating cellular behavior.

Some previous studies help to identify where FGFR4 fits in the pathway of differentiation. In chick, FGFR4 is expressed transiently, and follows up-regulation of Pax3. In mouse, FGFR4 has been found to be a direct transcriptional target of Pax3 (Lagha et al., 2008). Additionally, ectopic misexpression of Pax3 throughout the entire cranial ectoderm up-regulates FGFR4 expression, but does not lead to delamination or differentiation of these cells (Dude et al., 2009). This suggests that Pax3 leads to transient FGFR4 expression, but together they are not sufficient for opV placode development, and that additional signal transduction pathways must be activated for delamination and neuronal differentiation. An additional parallel pathway that may be critical to overall opV placode development is the canonical Wnt signaling pathway, which has also been shown to be necessary for Pax3 expression and maintenance of the opV placode fate (Lassiter et al., 2007).

The combinatorial requirement for multiple molecular pathways in placode development is not surprising. It has been shown that general placodal competence requires the activation of multiple signaling pathways in the very young embryo (Litsiou et al., 2005). In both the otic and epibranchial placodes, it has been shown that the interplay of canonical Wnt and FGF signals regulate the steps necessary for placode differentiation (Freter et al., 2008). In addition, it was recently reported that Wnt1 and FGF8, emanating from the midbrain–hindbrain boundary, work cooperatively to direct the establishment and differentiation of opV placode cells, and that FGF signaling, acting through the MAPK pathway, is necessary to maintain early neuronal differentiation of opV placode cells (Canning et al., 2008). This study also showed that although overactivating Wnts and FGFs in the neural tube did lead to premature differentiation of opV neurons, ectopic neurons were never generated outside the normal placode domain. This could explain why we did not observe an expansion of the placode after ectopic FGF8 expression alone. While our data did not evaluate the role of FGF signaling in placode induction, we similarly showed that FGF signaling is required for the progression of opV placode cells through the differentiation process, even in specified (Pax3+) cells. This careful examination of the role of FGFR4 in opV placode development demonstrates that FGF signaling regulates cellular processes associated with delamination, which in turn impacts neuronal differentiation of opV placode cells.

Experimental Procedures

Expression Reagents

The secreted quail FGF receptor-4 (sFGFR4) was a kind gift from Christophe Marcelle (Marics et al., 2002). sFGFR4 was ligated into the RSV/pCL vector, which contains a separate SV40 promoter driving GFP (Scaal et al., 2004). The chicken cytoplasmic-truncated FGFR4 (tFGFR4) contains a C→T point mutation at nucleotide 1360 resulting in premature stop codon at amino acid 454 (CAG→TAG, Gln→Stop). The chicken FGF8 gene was obtained through polymerase chain reaction (PCR) amplification of cDNA (forward primer 5′-ATGGACCCCTGCTCCTCGCT-3′, reverse 5′-CACAATGTCTCTACGTCAGTCCA-3′). The resulting DNA fragment was ligated into RSV/pCL-GFP. The empty RSV/pCL-GFP vector was used as a control. All expression constructs were prepared for electroporation by resuspending at a concentration of 4–6 μg/μl in water with fast green added for visualization.

In Ovo Electroporation

Fertilized chicken (*Gallus gallus*) eggs were obtained from local farms and incubated to the desired stage in a humidified incubator at 38°C. The DNA constructs described above were electroporated into 7–9 ss chicken embryos using vertical electroporation, where the reference electrode was placed underneath the embryo through a small hole made outside the area opaca, and the driving electrode was placed directly above the area of interest (BTX 820 electroporator from Genetronics: five 10-ms pulses of 10 V each, one second gap between each pulse). Embryos were then allowed to develop for 24–36 hr before being harvested.

SU5402 Head Cultures

Head regions above the otic vesicle were dissected from 15 ss embryos using a micro-scalpel. Tissues were stored in complete medium on ice (10% fetal bovine serum, 2% chick embryonic extract in DMEM) until required, then rinsed in sterile DMEM before transplanting into collagen gels. Collagen matrix gels were prepared as previously described (Groves and Bronner-Fraser, 2000). Briefly, 90 μl of collagen solution and 10 μl of 10× DMEM were combined followed by addition of 4.5 μl of 7.5% sodium bicarbonate to adjust the pH to 7.5. Forty-microliter drops of the prepared collagen solution were plated and allowed to set. Head regions were then placed on top of collagen mound followed by 20 μl of collagen solution added to cover tissue. DMEM (1 ml) with N2 supplement (GIBCO) and antibiotic were added with either SU5402 (50 μM) or DMSO vehicle (adapted from Martin and Groves, 2006). Cultures were grown at 37°C and 5% CO_2 for 18 hr. Cultures were fixed in 4% formaldehyde for 3 hr at room temperature and prepared for cryosection. Sections were then immunostained and analyzed for Pax3 and Islet1 protein, as well as DAPI nuclear stain.

BrdU Labeling

Approximately 50 to 75μl of BrdU (1: 10, Zymed) was applied to embryos at 23 hr and 35 hr after electroporation. Embryos were then incubated at 37°C for 1 hr then harvested, fixed, and cryosectioned. Sections were rinsed in 0.1 M boric acid and subjected to 2 N HCl in phosphate buffered saline (PBS; 30 min at 37°C) followed by a PBS rinse 3× and wash (20 min).

Whole-Mount In Situ Hybridization

A chicken *Ngn2* DNA template was PCR amplified from chick cDNA using the following 3′-untranslated region–specific primers: Outer primers (forward 5′-GGGTCCAGGTTAGAAGTCATTG-3′ and reverse 5′-CACTGAGGGACATGGGTTAG-3′) and inner primers (forward 5′-GGCTTTGTCAGGGCTGAATG-3′ and reverse 5′-CACTGAGGGACATGGGTTAG-3′). The *Ngn2* digoxigenin (DIG) -labeled RNA probe was then synthesized and used for whole-mount in situ hybridization on chick embryos as described

by Henrique et al. (1995). Briefly, formaldehyde-fixed embryos of appropriate developmental stages were buffered and exposed to a DIG-labeled antisense RNA probe, which recognized the *Ngn2* mRNA transcripts. After removal of the nonspecifically adhering probe, the embryos were incubated with an alkaline phosphatase (AP) -labeled anti-DIG antibody, followed by a chromogenic substrate for AP.

Immunohistochemistry and Analysis

The following primary antibodies were used: Pax3 1:200 (mouse IgG2a; Baker et al., 1999), Pax2 1:200 (rabbit polyclonal; Zymed/Invitrogen), Pax6 1:200 (mouse IgG1; Developmental Studies Hybridoma Bank: DSHB), Islet-1 (mouse IgG2b; DSHB), Neurofilament 1:300 (mouse IgG1; DSHB), NeuN 1:100 (mouse IgG1; Chemi-con), BrdU (mouse IgG1; Sigma), GFP 1:500 (rabbit polyclonal; Invitrogen). The DSHB was developed under the auspices of the NICHD and is maintained by the University of Iowa, Department of Biological Sciences, Iowa City, IA 52242. Appropriately matched Alexa^{488}- 1:175, Alexa^{546}-1:1,000 or Alexa^{633}-1:175 conjugated goat anti-mouse or goat anti-rabbit secondary antibodies were obtained from Molecular Probes/Invitrogen. For immunohistochemistry on cryosections, embryos were embedded in gelatin and cryosectioned to generate 12-μm sections of the area of interest. Sections were mounted on Superfrost Plus glass slides and the gelatin removed by treating the slides in PBS at 37°C for 15–20 min. The slides were incubated overnight at 4°C in primary antibody, diluted in antibody buffer (PBS, 0.1% bovine serum albumen, 0.1% Tween), followed by incubation for 1 hr at room temperature in secondary antibodies diluted in antibody buffer. Three 5- to 10-min washes in PBS followed each incubation. Slides were mounted in Fluoromount G (SouthernBiotech). Sections were analyzed using epifluorescent microscopy; photographs from different channels were superimposed using Adobe Photoshop or Olympus Microsuite to observe overlapping expression.

For quantitative analysis, cells from five random sections of each opV placode/ganglion were analyzed to minimize variability and bias and averaged to produce a standard mean for each independent placode/ganglion (Lassiter et al., 2007). Embryos displaying obviously unhealthy tissue morphology were excluded from the data set, and only embryos where DAPI-stained nuclei were intact without any apparent degradation were included. Positive cells were determined and counted using Olympus Microsuite software to identify cells with minimum color thresholds. Statistical analysis was performed, with *P*-values calculated using Student's *t*-test to compare the standard means of control and experimental samples.

Supplementary Material

Refer to Web version on PubMed Central for supplementary material.

Acknowledgments

References

Bailey AP, Bhattacharyya S, Bronner-Fraser M, Streit A. Lens specification is the ground state of all sensory placodes, from which FGF promotes olfactory identity. Dev Cell 2006;11:505–517. [PubMed: 17011490]

Baker CV, Bronner-Fraser M. Establishing neuronal identity in vertebrate neurogenic placodes. Development 2000;127:3045–3056. [PubMed: 10862742]

Baker CV, Bronner-Fraser M. Vertebrate cranial placodes I. Embryonic induction. Dev Biol 2001;232:1– 61. [PubMed: 11254347]

Baker CV, Stark MR, Marcelle C, Bronner-Fraser M. Competence, specification and induction of Pax-3 in the trigeminal placode. Development 1999;126:147–156. [PubMed: 9834194]

Baker CV, Stark MR, Bronner-Fraser M. Pax3-expressing trigeminal placode cells can localize to trunk neural crest sites but are committed to a cutaneous sensory neuron fate. Dev Biol 2002;249:219–236. [PubMed: 12221003]

Begbie J, Ballivet M, Graham A. Early steps in the production of sensory neurons by the neurogenic placodes. Mol Cell Neurosci 2002;21:502–511. [PubMed: 12498790]

Bhattacharyya S, Bailey AP, Bronner-Fraser M, Streit A. Segregation of lens and olfactory precursors from a common territory: cell sorting and reciprocity of Dlx5 and Pax6 expression. Dev Biol 2004;271:403–414. [PubMed: 15223343]

Canning CA, Lee L, Luo SX, Graham A, Jones CM. Neural tube derived Wnt signals cooperate with FGF signaling in the formation and differentiation of the trigeminal placodes. Neural Dev 2008;3:35. [PubMed: 19077309]

Crossley PH, Martinez S, Martin GR. Midbrain development induced by FGF8 in the chick embryo. Nature 1996;380:66–68. [PubMed: 8598907]

D'Amico-Martel A, Noden DM. Contributions of placodal and neural crest cells to avian cranial peripheral ganglia. Am J Anat 1983;166:445–468. [PubMed: 6858941]

Dude CM, Kuan CY, Bradshaw JR, Greene ND, Relaix F, Stark MR, Baker CV. Activation of Pax3 target genes is necessary but not sufficient for neurogenesis in the ophthalmic trigeminal placode. Dev Biol 2009;326:314–326. [PubMed: 19100251]

Ericson J, Thor S, Edlund T, Jessell TM, Yamada T. Early stages of motor neuron differentiation revealed by expression of homeobox gene Islet-1. Science 1992;256:1555–1560. [PubMed: 1350865]

Faber SC, Dimanlig P, Makarenkova HP, Shirke S, Ko K, Lang RA. Fgf receptor signaling plays a role in lens induction. Development 2001;128:4425–4438. [PubMed: 11714669]

Freter S, Muta Y, Mak SS, Rinkwitz S, Ladher RK. Progressive restriction of otic fate: the role of FGF and Wnt in resolving inner ear potential. Development 2008;135:3415–3424. [PubMed: 18799542]

Ge W, He F, Kim KJ, Blanchi B, Coskun V, Nguyen L, Wu X, Zhao J, Heng JI, Martinowich K, Tao J, Wu H, Castro D, Sobeih MM, Corfas G, Gleeson JG, Greenberg ME, Guillemot F, Sun YE. Coupling of cell migration with neurogenesis by proneural bHLH factors. Proc Natl Acad Sci U S A 2006;103:1319–1324. [PubMed: 16432194]

Graham A, Blentic A, Duque S, Begbie J. Delamination of cells from neurogenic placodes does not involve an epithelial-to-mesenchymal transition. Development 2007;134:4141–4145. [PubMed: 17959723]

Groves AK, Bronner-Fraser M. Competence, specification and commitment in otic placode induction. Development 2000;127:3489–3499. [PubMed: 10903174]

Henrique D, Adam J, Myat A, Chitnis A, Lewis J, Ish-Horowicz D. Expression of a Delta homologue in prospective neurons in the chick. Nature 1995;375:787–790. [PubMed: 7596411]

Kuratani SC, Hirano S. The appearance of trigeminal ectopic ganglia within the surface ectoderm in the chick embryo. Arch Histol Cytol 1990;53:575–583. [PubMed: 2078402]

Ladher RK, Wright TJ, Moon AM, Mansour SL, Schoenwolf GC. FGF8 initiates inner ear induction in chick and mouse. Genes Dev 2005;19:603–613. [PubMed: 15741321]

Lagha M, Kormish JD, Rocancourt D, Manceau M, Epstein JA, Zaret KS, Relaix F, Buckingham ME. Pax3 regulation of FGF signaling affects the progression of embryonic progenitor cells into the myogenic program. Genes Dev 2008;22:1828–1837. [PubMed: 18593883]

Lassiter RNT, Dude CM, Reynolds SB, Winters NI, Baker CV, Stark MR. Canonical Wnt signaling is required for ophthalmic trigeminal placode cell fate determination and maintenance. Dev Biol 2007;308:392–406. [PubMed: 17604017]

Litsiou A, Hanson S, Streit A. A balance of FGF, BMP and WNT signalling positions the future placode territory in the head. Development 2005;132:4051–4062. [PubMed: 16093325]

Marcelle C, Eichmann A, Halevy O, Breant C, Le Douarin NM. Distinct developmental expression of a new avian fibroblast growth factor receptor. Development 1994;120:683–694. [PubMed: 8162862]

Marics I, Padilla F, Guillemot JF, Scaal M, Marcelle C. FGFR4 signaling is a necessary step in limb muscle differentiation. Development 2002;129:4559–4569. [PubMed: 12223412]

Martin K, Groves AK. Competence of cranial ectoderm to respond to FGF signaling suggests a two-step model of otic placode induction. Development 2006;133:877–887. [PubMed: 16452090]

McCabe KL, Bronner-Fraser M. Essential role for PDGF signaling in ophthalmic trigeminal placode induction. Development 2008;135:1863–1874. [PubMed: 18417621]

Mulder H, Leckstrom A, Uddman R, Ekblad E, Westermark P, Sundler F. Islet amyloid polypeptide (amylin) is expressed in sensory neurons. J Neurosci 1995;15:7625–7632. [PubMed: 7472513]

Mullen RJ, Buck CR, Smith AM. NeuN, a neuronal specific nuclear protein in vertebrates. Development 1992;116:201–211. [PubMed: 1483388]

Nechiporuk A, Linbo T, Poss KD, Raible DW. Specification of epibranchial placodes in zebrafish. Development 2007;134:611–623. [PubMed: 17215310]

Nikaido M, Doi K, Shimizu T, Hibi M, Kikuchi Y, Yamasu K. Initial specification of the epibranchial placode in zebrafish embryos depends on the fibroblast growth factor signal. Dev Dyn 2007;236:564–571. [PubMed: 17195184]

Perez SE, Rebelo S, Anderson DJ. Early specification of sensory neuron fate revealed by expression and function of neurogenins in the chick embryo. Development 1999;126:1715–1728. [PubMed: 10079233]

Sai X, Ladher RK. FGF signaling regulates cytoskeletal remodeling during epithelial morphogenesis. Curr Biol 2008;18:976–981. [PubMed: 18583133]

Scaal M, Gros J, Lesbros C, Marcelle C. In ovo electroporation of avian somites. Dev Dyn 2004;229:643–650. [PubMed: 14991719]

Schlosser G. Induction and specification of cranial placodes. Dev Biol 2006;294:303–351. [PubMed: 16677629]

Stark MR, Sechrist J, Bronner-Fraser M, Marcelle C. Neural tube-ectoderm interactions are required for trigeminal placode formation. Development 1997;124:4287–4295. [PubMed: 9334277]

Streit A. Early development of the cranial sensory nervous system: from a common field to individual placodes. Dev Biol 2004;276:1–15. [PubMed: 15531360]

Sun SK, Dee CT, Tripathi VB, Rengifo A, Hirst CS, Scotting PJ. Epibranchial and otic placodes are induced by a common Fgf signal, but their subsequent development is independent. Dev Biol 2007;303:675–686. [PubMed: 17222818]

Xu H, Dude CM, Baker CV. Fine-grained fate maps for the ophthalmic and maxillomandibular trigeminal placodes in the chick embryo. Dev Biol 2008;317:174–186. [PubMed: 18367162]
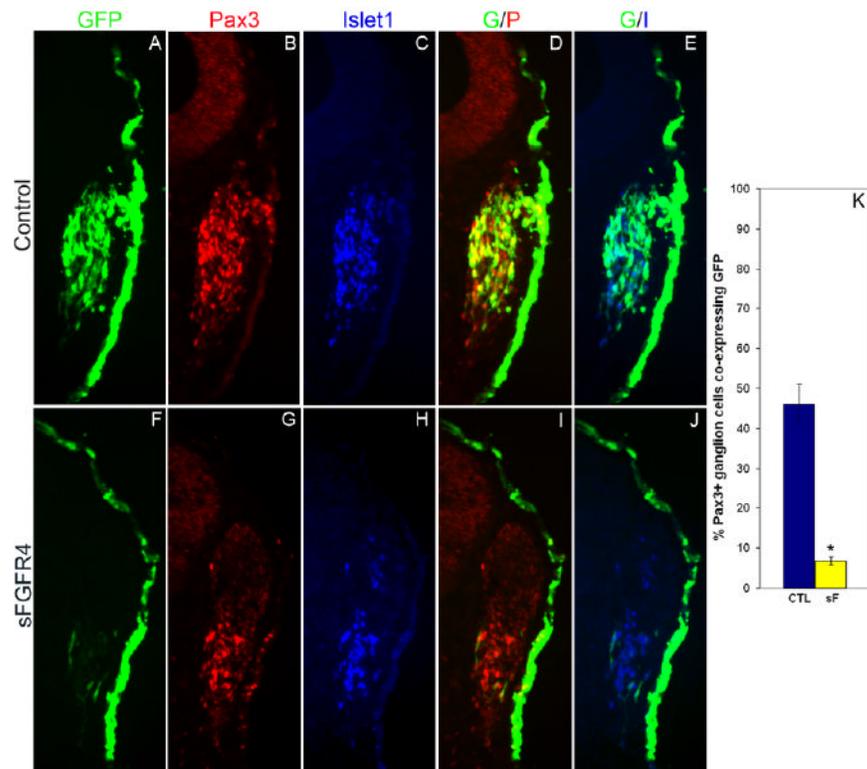
Fig. 1.
Blocking fibroblast growth factor (FGF) signaling prevents targeted cells from delaminating and contributing to the ophthalmic trigeminal (opV) ganglion. **A–J:** Transverse section through the opV ganglion region of a ~31 somite stage (ss) embryo collected 36 hr after electroporation at the 7–9 ss with the control green fluorescent protein (GFP) vector (A–E) or secreted-FGFR4 misexpression construct (sFGFR4; F–J). GFP expression (green) marks targeted cells, with immunostaining for Pax3 (red; B,G) and Islet1 (blue; C,H) shown in adjacent panels. D: Merged image of GFP and Pax3; cells targeted with the control plasmid express GFP and contribute substantially to the opV ganglion, with numerous cells expressing both GFP and Pax3 (yellow) in the mesenchyme with a few coexpressing cells remaining in the ectoderm. E: Merged image of GFP and Islet1; GFP+ cells coexpress with the neuronal marker Islet1 only in the mesenchyme (aqua). I: Merged image of sFGFR4 (green) and Pax3 (red); the majority of GFP+ sFGFR4-targeted cells remain in the ectoderm, do not express Pax3, and do not contribute to the ganglion, although a significant number of untargeted Pax3+ ganglionic cells are present, with a few Pax3+/GFP coexpressing cells in the ectoderm. J: Merged image of sFGFR4 (green) and Islet 1 (blue); sFGFR4 GFP+ cells remain in ectoderm and do not express Islet1. **K:** Histogram showing the percentage of Pax3+ ganglion cells coexpressing GFP (n = 8) or sFGFR4 (n = 9). Error bars depict SEM. The dramatic reduction in the contribution of Pax3+ sFGFR4-targeted cells to the ganglion is highly statistically significant ($P < 0.0001$).
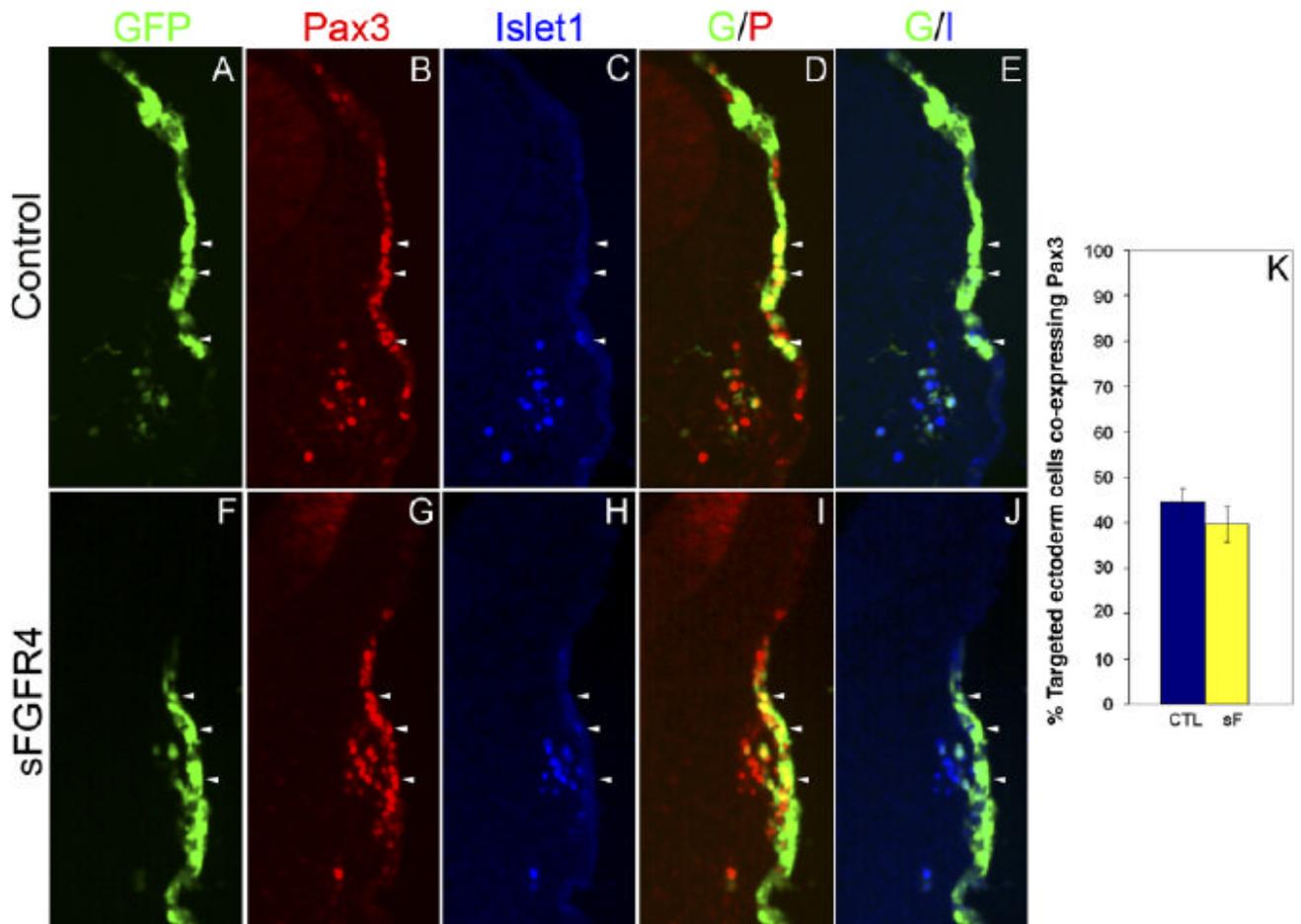
Fig. 2.
Inhibition of fibroblast growth factor receptor-4 (FGFR4) does not result in early loss of Pax3 expression in the ophthalmic trigeminal (opV) placode. **A–J:** Transverse section through the opV ganglion region of a ~24 somite stage (ss) embryo, 24 hr after electroporation at the 7–9 ss with GFP (A–E) or sFGFR4 (F–J) (green), immunostained for Pax3 (red; B,G) and Islet1 (blue; C,H). D: Merged image of green fluorescent protein (GFP) and Pax3. Cells targeted with the control plasmid coexpress GFP and Pax3 (yellow) in the ectoderm, with a few Pax3+ cells beginning to migrate into the mesenchyme. E: Merged image of GFP and Islet1; Islet1 is not expressed in the ectoderm, but is expressed in the mesenchyme with some cells coexpressing GFP and Islet1 (aqua). I: Merged image of secreted-FGFR4 misexpression construct (sFGFR4; green) and Pax3 (red). Cells targeted with sFGFR4 continue to express Pax3 (yellow) in the ectoderm. J: Merged image of sFGFR4 (green) and Islet1 (blue). Islet1 expression in the ectoderm is not up-regulated. Arrowheads demarcate the same cell through each panel. **K:** Histogram showing the percentage of targeted ectoderm cells coexpressing Pax3, in control (n = 6) vs. sFGFR4-targeted (n = 6) embryos. Error bars depict SEM. The difference between experimental and controls is not statistically significant ($P < 0.40$).
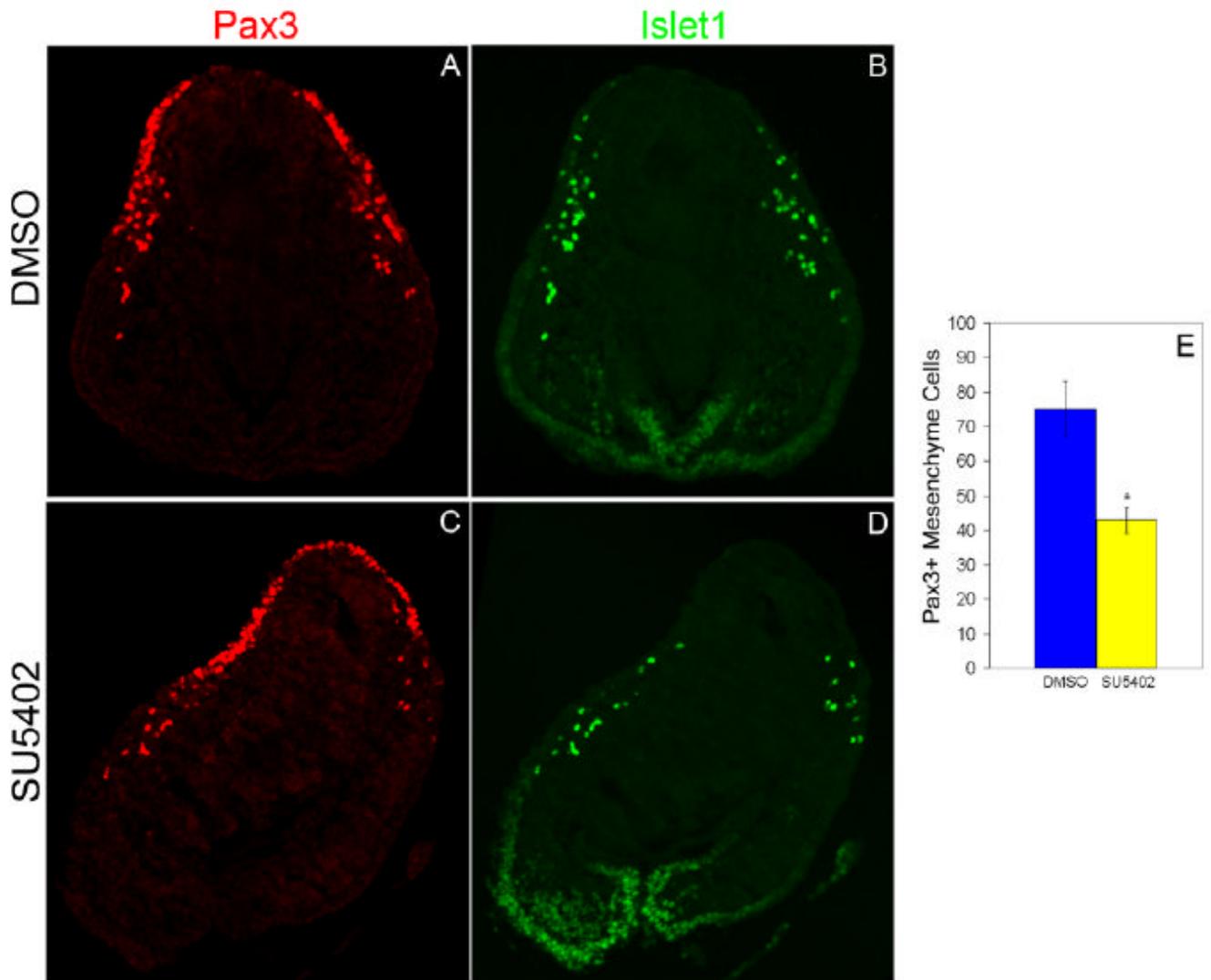
Fig. 3.
Blocking fibroblast growth factor (FGF) signaling prevents cells from delaminating and contributing to the mesenchyme. Transverse section through the ophthalmic trigeminal (opV) placode region of a 15 somite stage (ss) embryo cultured for 18 hr to approximately the 27 ss. Embryo head was cultured in either dimethyl sulfoxide (DMSO) or SU5402, immunostained for Pax3 (red; A, C) and Islet1 (green; B, D). **A,C:** In SU5402-cultured embryo heads, significantly fewer Pax3+ cells delaminate and migrate into the mesenchyme, whereas in DMSO-cultured embryos the cells continue to delaminate normally and move into the mesenchyme. **B,D:** Placode cells in SU5402 did not increase neuronal differentiation as shown by the scarce Islet-1 expression in the ectoderm. **E:** Histogram showing Pax3+ mesenchyme cells in DMSO (n = 7) or SU5402 (n = 9) embryos. Error bars depict SEM. The reduction in the number of Pax3+ cells in the mesenchyme of experimental embryos compared with controls is statistically significant ($P < 0.01$).
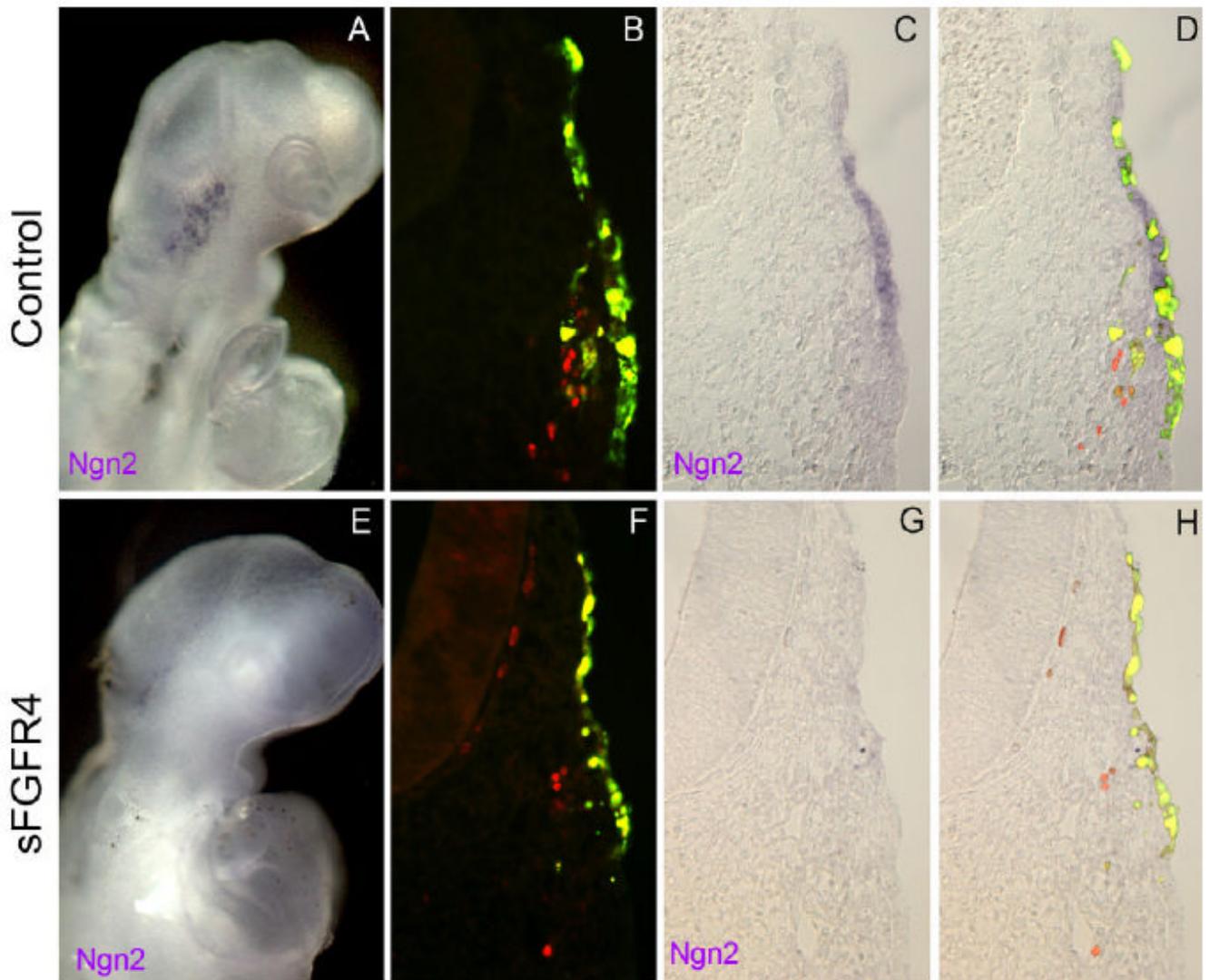
Fig. 4.
Inhibition of fibroblast growth factor (FGF) signaling results in a loss of the neuronal marker Ngn2. A,E: Whole-mount embryos collected and imaged 24 hr after electroporation at the 7–9 ss with RSV control vector (A) or secreted-FGF receptor-4 misexpression construct (sFGFR4; E). **A:** Whole-mount embryo electroporated with control RSV vector shows normal expression of the placode neuronal marker Ngn2. **B–D:** Transverse section through the ophthalmic trigeminal (opV) ganglion region of embryo electroporated with RSV control vector shows normal Ngn2 expression. **E:** Whole-mount embryo electroporated with sFGFR4 vector shows reduced expression of the placode neuronal marker Ngn2. **F–H:** Transverse section through the opV ganglion region of embryo electroporated with sFGFR4 control vector shows a loss of Ngn2 expression.
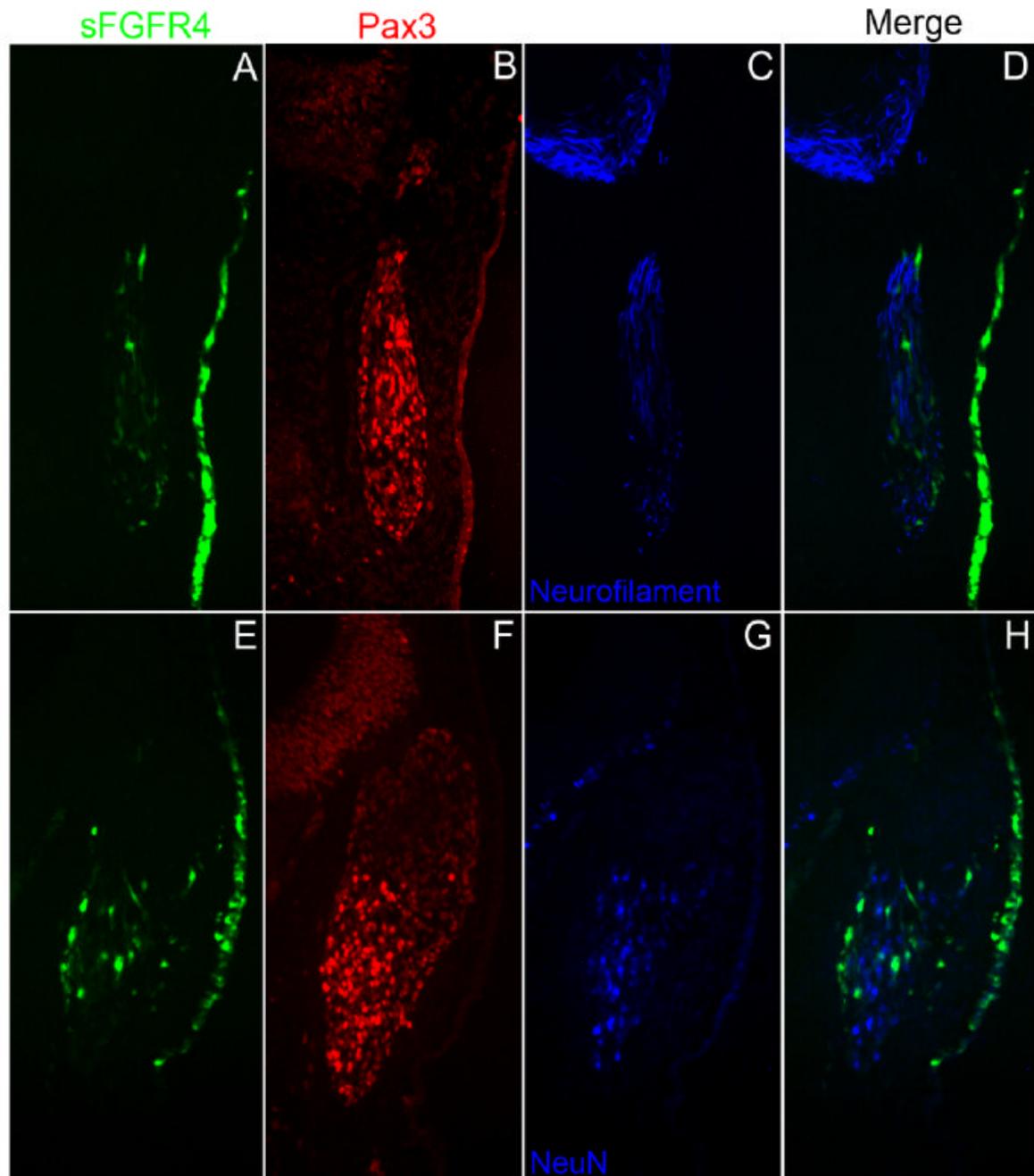
Fig. 5.
Secreted-fibroblast growth factor receptor-4 misexpression construct (sFGFR4) -targeted
ophthalmic trigeminal (opV) placode cells do not differentiate as neurons in the ectoderm. **A–
C,E–G:** Transverse section through the opV ganglion region of a ~31 somite stage (ss) embryo,
36 hr after electroporation at the 7–9 ss with sFGFR4 (green; A,E), immunostained for Pax3
(red; B,F), Neurofilament (blue; C), and NeuN (blue, G). **D:** Merged image of sFGFR4 (green)
and Neurofilament (blue). Cells in the ectoderm targeted with sFGFR4 do not up-regulate
Neurofilament, although the neuronal marker is still expressed in untargeted cells in the opV
ganglion. **H:** Merged image of sFGFR4 (green) and NeuN (blue); cells targeted with sFGFR4

do not delaminate and do not express the neuronal marker NeuN. Untargeted cells continue to migrate into the mesenchyme and express NeuN.
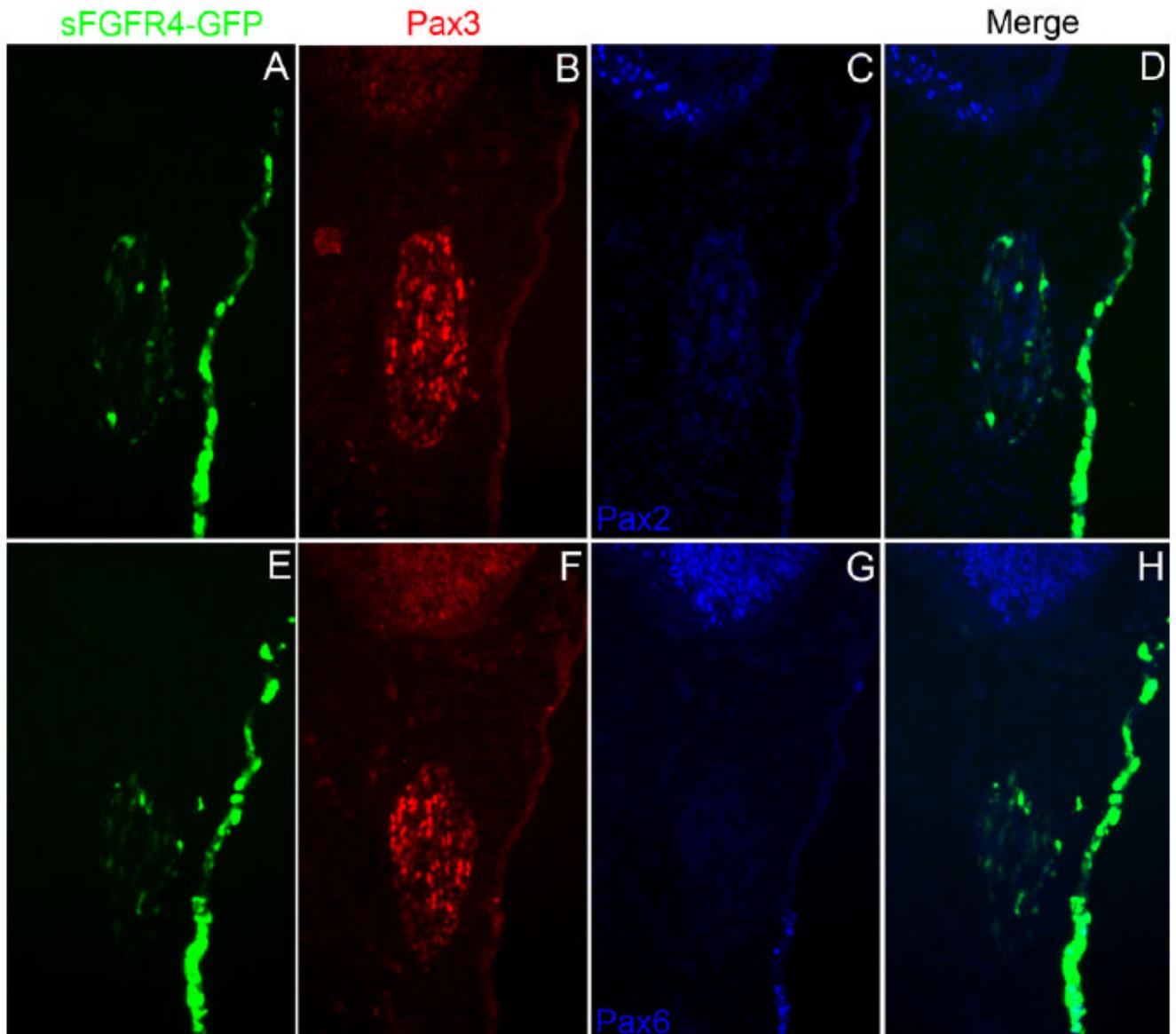
Fig. 6.
Ophthalmic trigeminal (opV) placode cells targeted with secreted-fibroblast growth factor receptor-4 misexpression construct (sFGFR4) do not express other placodal markers. **A–C,E– G:** Transverse section through the opV ganglion region of a ~31 ss embryo, 36 hr after electroporation at the 7–9 ss with the sFGFR4 vector (green, A,E), immunostained for Pax3 (red; B,F), Pax2 (blue, C), and Pax6 (blue, G). **D:** Merged image of sFGFR4 (green) and Pax2 (blue); cells targeted with sFGFR4 do not delaminate and do not up-regulate the epibranchial and otic marker Pax2. **H:** Merged image of sFGFR4 (green) and Pax6 (blue); targeted sFGFR4 cells do not up-regulate the lens placode marker Pax6 (Ectodermal expression near the bottom of H shows endogenous Pax6 expression near the lens placode).
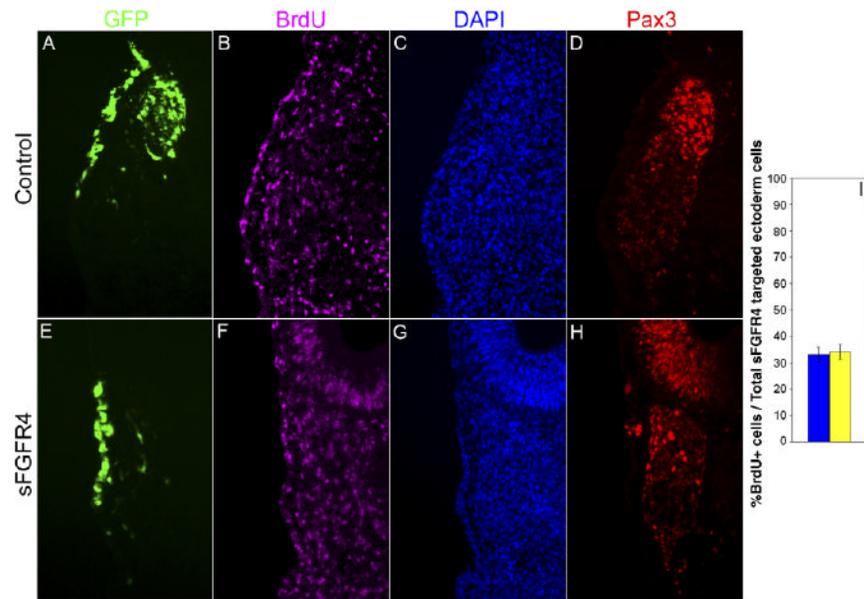
Fig. 7.
Blocking fibroblast growth factor (FGF) signaling does not alter the proliferative state of ophthalmic trigeminal (opV) placode cells. **A–H:** Transverse section through the opV ganglion region of a ~31 ss embryo, 36 hr after electroporation at the 7–9 ss with the secreted-FGF receptor-4 misexpression construct (sFGFR4) vector (green, A,E), immunostained for Pax3 (red, D,H), bromodeoxyuridine (BrdU; purple, B,F), and DAPI (4′,6-diamidine-2-phenylidole-dihydrochloride;blue, C,G). Cells targeted with sFGFR4 continue to proliferate in opV ectoderm compared with targeted control ectoderm cells. **I:** Histogram showing percentage of targeted ectoderm cells that were BrdU+/DAPI+ in control (n = 6) and experimental (n = 5) embryos. Error bars depict SEM. The difference between experimental and controls is not statistically significant ($P < 0.84$).